

See discussions, stats, and author profiles for this publication at: <https://www.researchgate.net/publication/44653681>

Packed DNA Denatures on Gold Nanoparticles

ARTICLE *in* THE JOURNAL OF PHYSICAL CHEMISTRY B · JULY 2010

Impact Factor: 3.3 · DOI: 10.1021/jp104533q · Source: PubMed

CITATIONS

12

READS

17

3 AUTHORS, INCLUDING:



[Ron Naaman](#)

Weizmann Institute of Science

304 PUBLICATIONS **5,354** CITATIONS

[SEE PROFILE](#)



[Shirley Shulman Daube](#)

Weizmann Institute of Science

43 PUBLICATIONS **884** CITATIONS

[SEE PROFILE](#)

Packed DNA Denatures on Gold Nanoparticles

Dana Peled,[†] Ron Naaman,^{*,†} and Shirley S. Daube[‡]

Department of Chemical Physics and Chemical Research Support, Weizmann Institute of Science, Rehovot 76100, Israel

Received: May 18, 2010; Revised Manuscript Received: May 20, 2010

Toward the construction of double stranded DNA-based biosensors, packing of thiolated double-stranded DNA adsorbed on gold nanoparticles was observed to induce DNA denaturation. The denaturation was investigated as a function of DNA density, nanoparticle surface area, and DNA length. Direct correlation was found between DNA surface coverage and the denaturation. Denaturation occurred only at high densities of adsorbed DNA and was dependent on DNA length and therefore stability, providing guidelines for controlled adsorption of dsDNA on GNPs. Our results invoke a model in which the formation of a thiol-gold bond competes with the free energy associated with the denaturation of two DNA strands. Denaturation vacates space for additional molecules to bind through a thiol-gold bond.

Introduction

Interactions between DNA and gold nanoparticles (GNPs) are playing a major role in biosensing and nanobiotechnology applications.^{1,2} GNPs have been used for labeling DNA,³ especially for the detection of mismatches during hybridization.^{4,5} Moreover, DNA has been used in combination with GNPs as a scaffold for the assembly of nanoscale building blocks to form artificial self-assembling nanostructures.^{1,6} All of these applications rely on sequence-selective hybridization of two complementary single-stranded DNA (ssDNA) to form stable double-stranded DNA (dsDNA). This is accomplished by first conjugating GNPs with ssDNA, followed by hybridization with a complementary ssDNA. However, direct conjugation of dsDNA to GNPs can expand the repertoire of sensing applications. For example, many DNA binding proteins recognize a specific site on dsDNA. Therefore, dsDNA can serve as an alternative to sequence detection by hybridization or for identification and quantification of DNA binding proteins. In addition, the activity of many DNA repair enzymes, related to human diseases, can only be monitored on dsDNA as a substrate.

The literature dealing with GNP-DNA interactions involves mostly adsorption of thiolated ssDNA on GNPs, followed by their hybridization, whereas dsDNA attached to GNPs was much less characterized. Almost no data are available regarding the conformation and stability changes that dsDNA molecules undergo upon their adsorption on surfaces or nanoparticles, despite the fact that this information is crucial for the design of dsDNA-based devices. The exception is the study in which short nonthiolated dsDNA has been shown to stabilize GNPs, most likely through denaturation of the dsDNA into its two ssDNA components, each adsorbing onto the surface of the GNPs.⁷

Recently, we developed a protocol for determining whether dsDNA oligomers adsorbed on a flat surface remained hybridized or had denatured.⁸ We approached this problem by placing a radiolabeled phosphate at the 5' end of one of two complementary oligomers (Figure 1). The radioactive phosphate was placed either on the strand harboring the thiol (thiolated) or on the complementary nonthiolated strand (complementary). Each

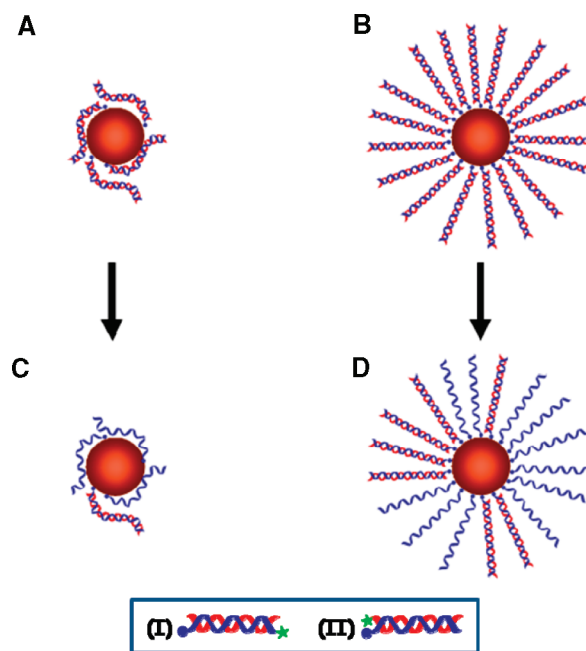


Figure 1. Possible mechanisms for dsDNA denaturation adsorbed on gold nanoparticles. At low concentrations of DNA, the dsDNA molecules may wrap around the particles but remain hybridized (A) or may interact with the surface leading to denaturation of the dsDNA (C). Alternatively, packing of DNA molecules on the GNP causes them to stretch (B) and denaturation of dsDNA may vacate more space for additional thiolated molecules to bind (D). In all cases, the thiolated strands remain on the particle, whereas the complementary nonthiolated strands are washed away. Inset: Two dsDNA species of the same sequences but with different strands harboring the radio label. (I) The strand modified with a thiol (blue circle) at the 3' end is labeled at the 5' end with a radioactive phosphate (green star) ("thiolated"). (II) The nonthiolated complementary strand (red) is labeled at the 5' end with a radioactive phosphate ("complementary").

of the radiolabeled strands was hybridized to its nonlabeled counterpart, resulting in two types of dsDNA species (Figure 1, insets I and II), that are chemically identical, except for the position of the radioactive phosphate.

We observed that 26 bp long dsDNA oligomers denatured very fast, following adsorption on flat gold surfaces, and that

* Corresponding author.

[†] Department of Chemical Physics.

[‡] Chemical Research Support.

the extent of denaturation of 50 bp long oligomers was much lower, suggesting that denaturation was inversely proportional to the stability of the dsDNA. We proposed two possible models that could account for this adsorption-dependent denaturation. In the first, denaturation stems from favorable interactions between the bases of the ssDNA and the surface.^{9,10} These nonspecific hydrophobic or electrostatic interactions of the bases with the surface may compete with the energy involved in hydrogen bonding and stacking of the bases within the dsDNA. When the gain in energy is higher because of the adsorption on the surface, denaturation may occur.^{11,12} In this scenario, the interaction of the DNA with the surface should be more pronounced at dilute monolayers, where more bare gold is exposed. A possible alternative model suggests that the denaturation of dsDNA on the surface is due to the formation of a dense layer. The area occupied by ssDNA on the surface is smaller than that of a dsDNA, as evident by the higher coverage of ssDNA compared with dsDNA monolayers.⁸ This may be due to the higher flexibility of ssDNA oligomers compared with the rigid rod structure of dsDNA molecules. In addition, ssDNA oligomers may undergo stretching and extension due to steric and electrostatic repulsion at the highly dense environment. Therefore, the denaturation allows for more thiolated DNA molecules to adsorb and additional thiol-gold bonds to be formed in the vacant space created upon double-strand dissociation. The results in ref 8 support the second model, in which the gain in energy due to the formation of a thiol-gold bond ($\Delta G \approx 40$ kcal/mol) overcomes the energy required to separate two DNA strands (ΔG at 25 °C, 0.4 M NaCl of 25.4, 39.9, and 85.9 kcal/mol for a 15, 26, and 50 bp long dsDNA, respectively), resulting in an observed denaturation of 95 and 85% for the 15 and 26 bp long DNA, respectively, and only 35% for the 50bp long.

This implies that the denaturation will be manifested only at high enough densities of DNA on the surface. To verify this model, a direct correlation between DNA density and denaturation is required. However, it is difficult to define quantitatively densities on surfaces where the nonhomogeneity in monolayer formation leads to an averaged density that may not accurately reflect the microscopic environment of individual DNA molecules.

A single nanoparticle has a maximal capacity to bind molecules, which depends on its surface area. Recently, Alivisatos and coworkers developed a gel electrophoresis assay, in which the density of ssDNA oligomers on GNPs can be directly determined by their distance of migration in an agarose gel.^{13–15} Here we extend this assay to dsDNA adsorbed on GNPs and use the correlation between gel migration and DNA density to probe the mechanism of adsorption-induced denaturation. By adsorbing dsDNA to GNPs at different molar ratios, it is possible to study the effect of density on the denaturation process. The initial DNA concentration in the DNA–GNP solution determines the density of the DNA on the GNP; therefore, we can easily produce a distribution of DNA/GNP with variable densities of adsorbates (Figure 1A,B). When relatively small amounts of DNA molecules are adsorbed, the DNA may be wrapped around the GNP (Figure 1A), but when the number of DNA molecules increases and the DNA becomes packed, the molecules most likely are in a stretched configuration (Figure 1B).¹³ If denaturation is induced by interactions with the gold surface, then the process progresses from species $A \rightarrow C \rightarrow D$ (in Figure 1), but if it is induced only by the high densities, the path of denaturation would follow $A \rightarrow B \rightarrow D$.

Our results verify that denaturation of dsDNA follows the latter path by demonstrating strand separation at the slow migration species in the gel. These species correspond to GNPs

covered with packed DNA. We show that the extent of denaturation could be modulated either by the radius of the GNP or by the length and, therefore, stability of the dsDNA.

Experimental Section

Gold Nanoparticles Preparation. GNPs (sigma) with an average diameter of either 5 or 10 nm were prepared as described previously by Alivisatos et al.¹⁶ In brief, to 1 mL citrate-coated GNPs (red solution), a 0.6 mg bis-(*p*-sulfonatophenyl) phenylphosphine dehydrate dipotassium salt (phosphine, Strem Chemicals) was added. Following overnight stirring at room temperature, several steps were required to get a suspended (red color) solution with phosphine-coated GNPs that can later be replaced by DNA. Solid NaCl was added to the GNPs mixture until GNP aggregation was achieved (as evident by the purple color). The aggregated GNPs were precipitated by centrifugation at room temperature for 20 min at 3500 rpm, the supernatant was removed, and the precipitated GNPs were resuspended in fresh phosphine solution (0.26 mg phosphine and 1 mL sterile deionized water) until the color turned red again. Salt was removed by an additional precipitation with methanol, and the precipitated GNPs were again resuspended in phosphine buffer. The concentration of GNPs in this final red solution was calculated by measuring the adsorption at 520 nm (Nano Drop).

DNA/Gold Nanoparticle Conjugation. Several solutions with increasing DNA concentrations (0.05–25 μ M) were prepared. Radiolabeled double-stranded DNA (26 and 50 bases pairs (bp) long) was added to a GNP solution with a final GNP concentration of $\sim 0.18 \mu$ M (or 1.1×10^{11} particles/ μ L) and supplemented with phosphine solution as above and NaCl to 50 mM. The mixtures were incubated for 2 h at room temperature while stirring before resolving by an agarose gel (2 or 3% agarose in $1 \times$ TAE). The gel was dried under vacuum overnight. The GNPs at this size have a deep red color and can be visualized in the gel. The gel was scanned by phosphorimager (FLA-5100, FUJI) to detect radioactive signals.

DNA Radiolabeling and Hybridization. DNA oligomers were labeled at their 5' end with 32 P using the enzyme T4 polynucleotide kinase and 32 P- γ -ATP according to published protocols.¹⁷ The radiolabeled single-stranded DNA were hybridized with their complementary nonlabeled strands at a ratio of 1:1.1 of thiolated-to-nonthiolated strands, respectively, to ensure that all of the thiolated strands are hybridized, as previously described.⁸ The oligomers were incubated at 80 °C for 10 min, following slow cooling to room temperature.

Radioactive Measurements. Agarose gels of GNPs adsorbed with radioactive DNA were exposed to a phosphorimaging screen, and the screen was imaged by a phosphorimager scanner (FLA-5100, FUJI). The amount of DNA that was bound to GNP was calculated from the radioactive signal. For every DNA concentration, the nonbound DNA and the bound DNA appear in the same lane. The percent of bound DNA for each DNA concentration was calculated from the total DNA in the lane.

The running distance was calculated by dividing the running distance of bound DNA by the running distance of the nonbound DNA, which was more or less equal for all DNA concentrations in the same gel. This calculation normalizes the migration distance and allows comparison between different gels.

The number of DNA molecules per GNP was calculated by dividing the number of bound DNA molecules (as was calculated from the radioactive signal in the gel) by the number of particles that were added to the reaction. On the basis of the gel analysis, most of the GNPs were bound by DNA.

Results and Discussion

Our goal has been to determine whether surface-induced DNA denaturation occurs at low or high DNA densities. If the denaturation process is induced by interactions with the gold surface, then it will be pronounced when only a few DNA molecules are adsorbed on each GNP, whereas if the denaturation is correlated with increased densities, then it will be observed when the DNA is packed (Figure 1).

In addition to having a well-defined DNA coverage, the technical advantage of using GNPs rather than flat gold surfaces is that fractionation of the bound DNA species can be done without washing but rather by resolving the various states of DNA by gel electrophoresis. Alivisatos et al. showed that the charge density of GNPs coated with phosphine is similar to that of DNA. Therefore, when DNA is adsorbed on GNPs, the DNA/GNP complex has an increased mass and size but the same charge density. The higher the mass and size of the complex, the more retarded is its migration in the gel. Therefore, not only does the gel resolve the DNA/GNP complexes from nonbound DNA but also the DNA-coated GNPs themselves are resolved to bands of GNPs with varying DNA densities.^{13,14}

Thiolated ssDNA (26 and 50 nucleotides long) were radio-labeled and hybridized with their complementary strands and were then attached at increasing concentrations to a fixed amount of phosphine-coated GNPs. Resolution of the GNPs–DNA solutions by electrophoresis on an agarose gel revealed retarded bands of DNA bound to GNP resolved from the fast migrating nonbound DNA (Figure 2A). The DNA/GNP complexes appeared as a distribution of discrete bands, where each of the bands represents a discrete number of DNA molecules bound to one GNP. The averaged DNA/GNP migration distance in the gel is therefore a direct indication of the DNA densities on the GNPs surfaces. The average migration distance decreased as the amount of DNA added to the GNPs increased (Figure 2B).

To probe directly the denaturation process, we compared the adsorption onto GNPs of the two DNA species that are chemically identical, except for the position of their radioactive labeling (Figure 1, inset). The radioactive signal of the bound DNA in the DNA/GNP complexes was monitored for each of the two DNA species as the DNA concentration in the solution was changed in the range 0.05–15 μM . Up to $\sim 2 \mu\text{M}$ DNA concentration, the two 26bp DNA species bound to the GNP to the same extent. However, as the concentration of DNA increased, the amount of the complementary nonthiolated strand appeared less in the bound complexes compared with the thiolated strand (Figure 2C).

The ratio between the radioactive signals from the two types of DNA/GNP is an indication of the level of denaturation, assuming that all nonthiolated DNA that is found in the DNA/GNP band is bound through hybridization to the thiolated DNA. This is a safe assumption because it has been shown that complexes composed of nonthiolated DNA physisorbed to GNPs do not sustain the electrophoretic field and migrate as nonbound DNA.¹⁵ If the adsorbed DNA remains in its original double-stranded conformation, then a ratio of unity between the radioactive measurements of the two species is expected. Any denaturation leading to loss of the complementary strand should result in a decrease in the signal obtained from species II but not from species I (Figure 1), resulting in a ratio of less than unity. Figure 2C clearly shows that for 26bp DNA, at solution concentrations $>2 \mu\text{M}$, the amount of labeled complementary strand that is bound to GNP was always lower than the

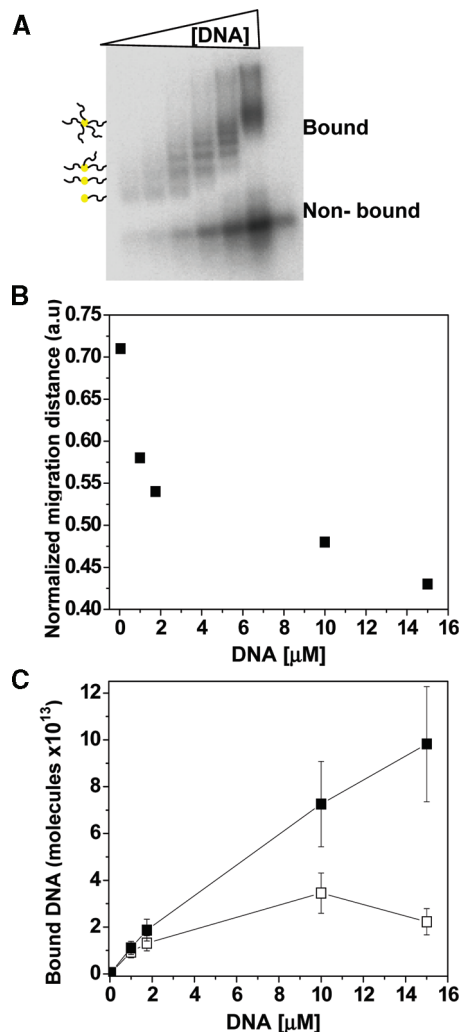


Figure 2. Separation of DNA bound to GNPs from nonbound DNA by agarose gel electrophoresis. (A) Autoradiogram of a 3% agarose gel of radiolabeled dsDNA, conjugated to GNP. The number of DNA molecules in the DNA/GNP complex increased with DNA concentration. By using gel electrophoresis the fraction of the nonbound DNA is separated from the complex without washing. (B) Normalized migration distance for each DNA concentration that was used in the DNA/GNP complexes as derived from the gel scan. (C) Number of radiolabel DNA molecules conjugated to 5 nm GNP as a function of DNA concentration (micrometers). The squares represent the two DNA species: thiolated (■) and complementary (□).

corresponding amount of the thiolated strands, indicating that denaturation had occurred.

The shift in gel migration of DNA/GNP complexes allowed us to relate directly the denaturation process to the GNP coverage, yielding, for the 26 bp DNA, 15–30% denaturation at low GNP/DNA coverage, and $\sim 80\%$ denaturation for DNA-saturated GNPs (Figure 3, ■).

If denaturation was indeed correlated with the surface area of the GNP, changing the radius of the GNP is expected to shift the denaturation to higher concentrations. We therefore adsorbed the same two DNA species to 10 nm rather than to 5 nm diameter GNPs. The DNA adsorption process was similar to that for the 5 nm, except that 15 μM DNA was needed to saturate the GNPs with adsorbed molecules. Denaturation was also evident for this size of GNPs but was more apparent at higher molar ratios of DNA/GNP (Figure 3A). To better demonstrate that for the two GNP sizes the denaturation actually depends on the surface density of DNA, we converted the molar

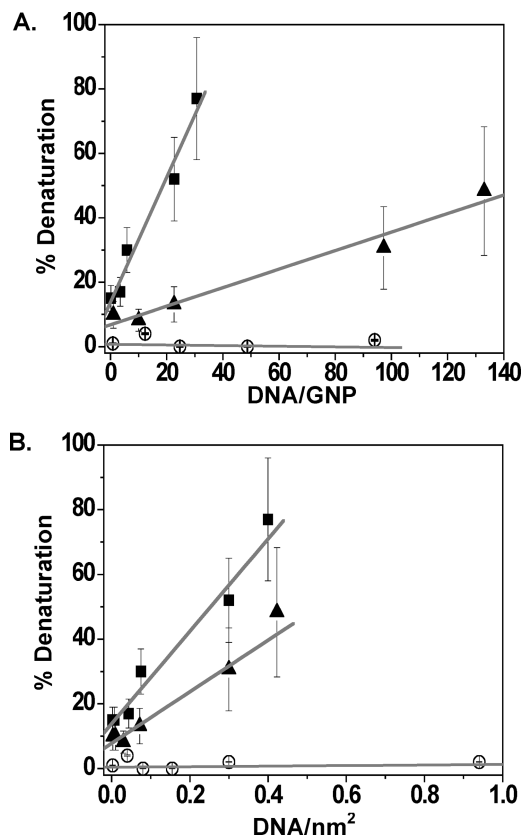


Figure 3. Denaturation as a function of DNA density. Percent of denaturation was plotted as a function of increasing DNA molecules per GNP for three types of DNA/GNP complexes: 26bp DNA conjugated to 5 nm GNP (■), 26bp DNA conjugated to 10 nm GNP (▲), and 50bp DNA conjugated to 10 nm GNP (○). Denaturation was plotted as a function of (A) the molar ratio between DNA strands and GNP and (B) the number of DNA strands per available GNP surface area.

ratio of DNA/GNPs to a surface area density. This was done by dividing each ratio with the corresponding surface area of the 5 and 10 nm GNP, $4\pi(2.5)^2$, and $4\pi(5)^2$, respectively. Replotting the data yielded two linear dependencies with similar slopes, with a ratio of 1.8 between the slopes (Figure 3B). Therefore, we conclude that the extent of DNA denaturation is proportional to the occupied surface area on the GNP.

According to our model, denaturation at high densities of adsorbed DNA occurs because it vacates space for more thiolated strands to bind, resulting in gain in free energy. This suggests that DNA denaturation would depend on the stability of the DNA in comparison to the stability of a thiol/gold bond.⁸ By replacing the 26bp DNA oligomers with 50 bp DNAs (Figure 3A,B, ○), we could demonstrate that almost no denaturation was observed at all DNA/GNP ratios. Consistent with our model, the gain in energy from an additional thiol/gold bond is no longer sufficient to compensate for the loss of energy involved in separation of 50bp long DNA strands.

Conclusions

The results presented here confirm that surface-induced denaturation occurs at high DNA densities. At low densities,

even though the DNA is most likely wrapped around the GNP, the hydrogen bonds and base stacking that stabilize the double strand are stronger and compete with nonspecific interactions between the bases and the gold. Denaturation occurs when the system becomes dense, and the release of the nonthiolated strand allows more thiolated strands to bind. This is fully consistent with our observation that an almost identical linear dependence of denaturation on surface area was obtained for two different sizes of GNPs (Figure 3B).

The use of GNPs in this study allowed us to reach firmer conclusions regarding the mechanism responsible for DNA denaturation of surfaces. The experiments do not require a washing process, which may increase the experimental error. In addition, the use of GNPs with variable sizes and a gel analysis provided us with the means to make a direct correlation with the adsorbates' density rather than calculating the averaged density on a flat surface. Finally, this investigation provides guidelines for adsorbing dsDNA on GNPs: At low densities, 20–30 long DNA oligomers can be used, with only ~10% expected denaturation. When higher densities are required, dsDNA longer than 50 bp should be used to minimize denaturation.

Acknowledgment. This work was partially supported by the Grand Center at the Weizmann Institute and the Israel Science Foundation.

References and Notes

- (1) Parak, W. J.; Gerion, D.; Pellegrino, T.; Zanchet, D.; Micheel, C.; Williams, S. C.; Boudreau, R.; Le Gros, M. A.; Larabell, C. A.; Alivisatos, A. P. *Nanotechnology* **2003**, *14*, R15–R27.
- (2) Storhoff, J. J.; Mirkin, C. A. *Chem. Rev.* **1999**, *99*, 1849–1862.
- (3) Taton, T. A.; Mirkin, C. A.; Letsinger, R. L. *Science* **2000**, *289*, 1757–1760.
- (4) Maruccio, G.; Primiceri, E.; Marzo, P.; Arima, V.; Della Torre, A.; Rinaldi, R.; Pellegrino, T.; Krahne, R.; Cingolani, R. *Analyst* **2009**, *134*, 2458–2461.
- (5) Sato, K.; Hosokawa, K.; Maeda, M. *J. Am. Chem. Soc.* **2003**, *125*, 8102–8103.
- (6) Yao, H.; Yi, C. Q.; Tzang, C. H.; Zhu, J. J.; Yang, M. S. *Nanotechnology* **2007**, *18*, 015102.
- (7) Yang, J.; Pong, B. K.; Lee, J. Y.; Too, H. P. *J. Inorg. Biochem.* **2007**, *101*, 824–830.
- (8) Peled, D.; Daube, S. S.; Naaman, R. *Langmuir* **2008**, *24*, 11842–11846.
- (9) Storhoff, J. J.; Elghanian, R.; Mirkin, C. A.; Letsinger, R. L. *Langmuir* **2002**, *18*, 6666–6670.
- (10) Wolf, L. K.; Gao, Y.; Georgiadis, R. M. *Langmuir* **2004**, *20*, 3357–3361.
- (11) Michalek, X. *Nano Lett.* **2001**, *1*, 341–343.
- (12) Opdahl, A.; Petrovykh, D. Y.; Kimura-Suda, H.; Tarlov, M. J.; Whitman, L. J. *Proc. Natl. Acad. Sci. U.S.A.* **2007**, *104*, 9–14.
- (13) Parak, W. J.; Pellegrino, T.; Micheel, C. M.; Gerion, D.; Williams, S. C.; Alivisatos, A. P. *Nano Lett.* **2003**, *3*, 33–36.
- (14) Zanchet, D.; Micheel, C. M.; Parak, W. J.; Gerion, D.; Alivisatos, A. P. *Nano Lett.* **2001**, *1*, 32–35.
- (15) Zanchet, D.; Micheel, C. M.; Parak, W. J.; Gerion, D.; Williams, S. C.; Alivisatos, A. P. *J. Phys. Chem. B* **2002**, *106*, 11758–11763.
- (16) Loweth, C. J.; Caldwell, W. B.; Peng, X. G.; Alivisatos, A. P.; Schultz, P. G. *Angew. Chem., Int. Ed.* **1999**, *38*, 1808–1812.
- (17) Aqua, T.; Naaman, R.; Daube, S. S. *Langmuir* **2003**, *19*, 10573–10580.

JP104533Q